

Magnetocaloric effect of $\text{Co}_{62}\text{Nb}_6\text{Zr}_2\text{B}_{30}$ amorphous alloys obtained by mechanical alloying or rapid quenching

L. M. Moreno, J. S. Blázquez, J. J. Ipus,^{a)} J. M. Borrego, V. Franco, and A. Conde
Dpto. Física de la Materia Condensada, ICMSE-CSIC, Universidad de Sevilla, P.O. Box 1065, 41080 Sevilla, Spain

(Presented 6 November 2013; received 22 September 2013; accepted 10 October 2013; published online 6 January 2014)

Amorphous samples of nominal composition $\text{Co}_{62}\text{Nb}_6\text{Zr}_2\text{B}_{30}$ have been prepared using mechanical alloying (MA) and rapid quenching (RQ) techniques. Differences appear in Curie temperature and the phases developed after crystallization. Refrigerant capacity is enhanced 20% in the MA-sample with respect to that of RQ-sample. Neglecting the demagnetizing factor of powder samples significantly affects the exponent n characterizing the field dependence of the maximum magnetic entropy change. © 2014 AIP Publishing LLC. [<http://dx.doi.org/10.1063/1.4857595>]

I. INTRODUCTION

Amorphous and nanocrystalline soft magnetic alloys have deserved the attention of the research community as these metastable microstructures lead to the disappearance¹ or averaging out^{2,3} of the magnetocrystalline anisotropy. Moreover, additional reduction of magnetoelastic anisotropy can be obtained in some compositions after certain field and thermal treatments making this type of materials the softest magnetic materials known.⁴

In recent years, these soft magnetic materials have also been studied as candidates for room temperature magnetic refrigeration as they present a second order phase transition with negligible hysteresis and they lack of rare earth elements, which significantly reduces the cost.⁵ In fact, magnetic refrigeration based on magnetocaloric effect (MCE) at room temperature is a promising technology with environmental and efficiency advantages over the conventional systems based on compression-expansion of gasses.

Although the conventional way to produce amorphous alloys is via rapid quenching (RQ) from a liquid melt with suitable composition (close to an eutectic),⁴ mechanical alloying (MA) (generally ball milling) has been shown as a versatile technique which also leads to the formation of amorphous structures and even with a broader compositional range than that can be obtained by rapid quenching.⁶

In this work, two amorphous samples of the same nominal composition $\text{Co}_{62}\text{Nb}_6\text{Zr}_2\text{B}_{30}$ have been prepared from mechanical alloying and melt-spinning techniques, respectively. Differences in microstructure, magnetization, and MCE are studied.

II. EXPERIMENTAL

Two samples with $\text{Co}_{62}\text{Nb}_6\text{Zr}_2\text{B}_{30}$ nominal composition were prepared by two different methods: mechanical alloying of elemental powders and rapid quenching. The mechanically alloyed sample, MA-sample, was prepared by ball milling during 40 h at 350 rpm (frequency ratio -2) in a

planetary mill Fritsch Pulverisette 4 Vario from a mixture of elemental powders. The initial powder mass was 5 g and the ball to powder ratio was 10:1. Further details on the milling process can be found elsewhere.⁷ The rapidly quenched sample, RQ-sample, was obtained by single-roller melt-spinning technique where the alloy ingots were prepared from high purity elements by arc melting under argon atmosphere.

X-ray diffraction (XRD) patterns were recorded at room temperature in a Bruker D8I diffractometer using Cu K α radiation for the MA-sample and in a Philips PW 1820 diffractometer using Co K α radiation for the RQ-sample. The thermal stability of the samples was studied by differential scanning calorimetry (DSC) in a Perkin-Elmer DSC7 under Ar flow. The magnetic properties were studied using a Lakeshore 7407 vibrating sample magnetometer (VSM) using a maximum applied magnetic field $H = 1.5$ T. The magnetic entropy change due to the application of a magnetic field has been calculated using a numerical approximation to the equation,

$$\Delta S_M = \int_0^{H_{max}} \left(\frac{\partial M}{\partial T} \right)_H dH, \quad (1)$$

where ΔS_M is the magnetic entropy change, M is the magnetization, and T is the temperature. Values of the Curie temperature, T_C , were estimated as the inflexion point of the $M(T)$ curves at $H = 0.05$ T.

III. RESULTS AND DISCUSSION

XRD patterns for as-milled MA and as-cast RQ samples are shown in Figures 1(a) and 1(c), respectively. Although both XRD patterns show typical amorphous haloes, previous XRD and scanning electron microscopy, SEM, studies⁷ confirmed that the microstructure of MA-sample is composed of ~90% of amorphous phase with dispersed hcp-Co nanocrystals of about 5 nm in size and boron inclusions of ~100 nm in size. About 4 at. % of Fe due to contamination from milling media was found by energy dispersive X-ray (EDX) spectroscopy. The RQ-sample presents slight surface

^{a)}Electronic mail: jhonipus@us.es.

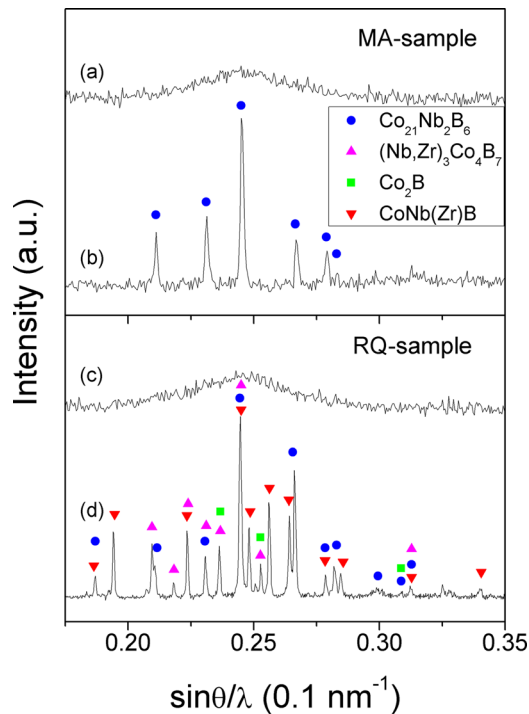


FIG. 1. XRD patterns for as-milled (a) and as-quenched (c) samples and for the same samples after crystallization, (b) and (d), respectively. The lines of the different crystalline phases are indicated.

crystallization that disappears after polishing. There is a single line at $d = 3.45 \text{ \AA}$ which prevents an unambiguous identification of the phase. However, this line could be ascribed to some oxide phase. DSC scans at 10 K/min (Figure 2) show several differences between the two studied samples. For the MA-sample two exothermic events appear: the first one, with a peak temperature $T_p = 670 \text{ K}$, corresponds to relaxation phenomena and the second one, with $T_p = 900 \text{ K}$, to crystallization. For the RQ-sample, relaxation phenomena, much less significant than for MA-sample, a glass transition at about 930 K and a single crystallization event with $T_p = 960 \text{ K}$ are observed.⁸ On the other hand, for the MA-sample, crystallization process produces a single fcc $\text{Co}_{21}\text{Nb}_2\text{B}_6$ -type phase (with metal to boron ratio 23:6), for the RQ-sample, besides this $\text{Co}_{21}\text{Nb}_2\text{B}_6$ -type phase, other B-rich boride phase have been detected: $\text{Co}(\text{Nb,Zr})\text{B}$, Co_2B (with metal to boron ratio of 2:1) and $(\text{Nb,Zr})_3\text{Co}_4\text{B}_7$ (with metal to boron ratio 1:1). Figures 1(b) and 1(d) show the XRD patterns of MA and RQ-samples after being heated at 10 K/min up to the end of the corresponding crystallization process (998 K and 1035 K for the MA and RQ-samples, respectively). The absence of boron rich phases in the crystallized MA-sample can be ascribed to a poorer B content of the amorphous phase developed by milling due to the remaining B-inclusions. In fact, a composition of $(\text{Co}_{62}\text{Nb}_6\text{Zr}_2)_{81}\text{B}_{19}$ can be estimated assuming a 23:6 metal to boron ratio for the amorphous phase in the MA-sample that yields the formation of a 23:6 intermetallic.

Figure 3(a) shows the temperature dependence of the specific magnetization at 0.05 T for both amorphous samples. From these curves, $T_C = 530 \text{ K}$ and 210 K were obtained for the MA and RQ-samples, respectively. This significant

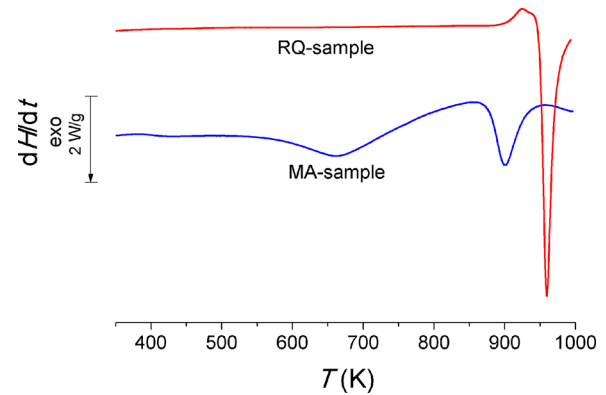


FIG. 2. DSC scans at heating rate of 10 K/min for as-milled and as-quenched samples.

difference in the Curie temperature can be also ascribed to the presence of B inclusions in the MA-sample, i.e., to a reduced B content in the amorphous phase. In fact, T_C decreases about 30 K/at. % B for $\text{Co}_{100-x}\text{B}_x$ alloys.⁹ Therefore, the estimated composition of the amorphous matrix should be $(\text{Co}_{62}\text{Nb}_6\text{Zr}_2)_{81}\text{B}_{19}$, which is in good agreement with our previous estimation. The agreement could even be enhanced after taking into account that there is a small amount of Fe from contamination coming from the milling media in the MA-sample ($\sim 4 \text{ at. \%}$ Fe), which also contributes to increasing the Curie temperature for Co-based amorphous alloys.

Figure 3(b) shows the temperature dependence of magnetic entropy change, $\Delta S_M(T)$, for the milled and quenched

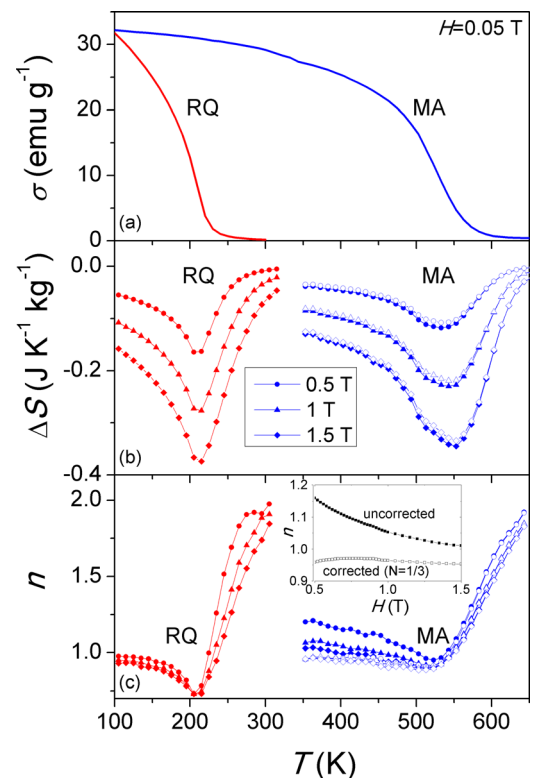


FIG. 3. Temperature dependences of specific magnetization at $H = 0.05 \text{ T}$ (a), magnetic entropy change (b), and exponent n (c) at maximum fields of $H = 0.5, 1, \text{ and } 1.5 \text{ T}$. The inset shows the field dependence of n at $T = 330 \text{ K}$ for uncorrected ($N = 0$) and corrected ($N = 1/3$) values.

samples. The minimum in $\Delta S_M(T)$ is shifted to higher temperatures in the MA-sample with respect to that of RQ-sample as it occurs for T_C values. Although the value of this minimum does not change significantly, the MCE peak broadens for the MA-sample with respect to the RQ-sample, leading to a 20% enhancement in the refrigerant capacity estimated as the product of the maximum $|\Delta S_M|$ times the full width at half maximum. Figure 3(c) shows the temperature dependence of the exponent n characterizing the field dependence of the magnetic entropy change: $\Delta S_M = aH^n$. For the RQ-sample, $n(T)$ curves are similar to those previously observed for other amorphous alloys¹⁰ with three temperature regimes where n is field independent. A ferromagnet well below T_C shows $n = 1$ and a paramagnet well above T_C shows $n = 2$. At T_C , n is independent of the field and takes a value of ~ 0.74 , similar to those found for other amorphous alloys¹¹ and which is related to the critical exponents (δ and β) as

$$n = 1 + \frac{1}{\delta} \left(1 - \frac{1}{\beta} \right), \quad (2)$$

whereas β exponent describes the evolution of M with $T - T_C$ at $H = 0$ and δ describes the evolution at T_C of M with H . Therefore, the effect of the demagnetizing factor should be concentrated in δ exponent.

However, $n(T)$ for the MA-sample exhibits a very different behavior (although similar to that found for other ball milled samples).^{12,13} At low temperatures, $n > 1$ and shows a strong field dependence even at T_C , where $n(T_C) = 0.905$, well above the value observed for the RQ-sample. There is a main factor which has not usually considered in the calculation of ΔS_M (and thus in the calculation of n) using Eq. (1), the demagnetizing factor, N .¹⁴ In fact, for a square ribbon sample of ~ 3 mm in wide and ~ 20 μm thick, $N = 0$ is a good approximation. However, for powder samples, by assuming that the particles are spherical, N should be $1/3$. We have to take that the field in Eq. (1) should be the internal field $H^{int} = H - NM$. Therefore, H^{int} has been calculated from each $M(H)$ curve and the different $M(H)$ curves obtained in the VSM were transformed into $M(H^{int})$ data. Corrected values of $\Delta S_M(T)$ and $n(T)$ plots considering $N = 1/3$ are also shown in Figures 3(b) and 3(c), respectively, as hollow symbols. It is worth noting that $\Delta S_M(T)$ plots for the MA-sample are not significantly affected but just a very slight reduction in ferromagnetic range is observed. However, $n(T)$ curves are strongly modified after considering $N = 1/3$ for powder samples. The main difference is observed at low temperatures where field independent $n = 1$ values are recovered, as it should correspond to a ferromagnetic sample well below its Curie temperature. Moreover, $n(T_C)$ becomes also practically field independent and its value is reduced with respect to those obtained from ΔS_M calculated using Eq. (1). However, this value $n(T_C) = 0.895$ is still clearly higher than those found for ribbon samples of amorphous alloys, for which $N \sim 0$. A possible explanation of this higher value is the existence of a broader distribution of Curie temperatures in the MA-sample compared to that of RQ-sample. The slope observed at the inflexion point in $M(T)$ curves of Figure 3(a) is in agreement with this proposed distribution of

Curie temperature as dM/dT values at T_C are -0.25 and -0.45 $\text{emu g}^{-1} \text{K}^{-1}$ for the MA and RQ-samples, respectively. A broader distribution of T_C should lead to a flattened and smaller minimum for $n(T)$. Instead of the theoretical $n(T_C)$ value predicted by Eq. (2), an average of the $n(T)$ values around T_C should be observed. This is in agreement with the observed $n(T)$ curve for the MA-sample.

IV. CONCLUSIONS

Two amorphous samples of nominal composition $\text{Co}_{62}\text{Nb}_6\text{Zr}_2\text{B}_{30}$ were prepared by mechanical alloying and rapid quenching techniques, respectively. Boron inclusions observed in the MA-sample implies a lower B content than the nominal one for the amorphous phase developed by mechanical alloying, which is estimated as $(\text{Co}_{62}\text{Nb}_6\text{Zr}_2)_{80}\text{B}_{20}$. This poorer boron content of the amorphous phase of the MA-sample explains the much higher value of the T_C in this sample than in the RQ-sample as well as the lack of B-rich intermetallic compounds as a product of crystallization. The MA-sample shows a broader distribution of T_C in the amorphous phase than the RQ-sample.

On the other hand, the maximum absolute value of ΔS_M is similar for both samples, refrigerant capacity is enhanced $\sim 20\%$ in the MA-sample with respect to that of RQ-sample due to the broad distribution of Curie temperatures. The demagnetizing factor N for powder samples does not significantly affect the values of ΔS_M . However, when N is neglected, the exponent n characterizing the field dependence of ΔS_M is seriously affected leading to unrealistic values and artificial field dependences of this parameter. The broader distribution of Curie temperatures in the MA-sample should explain the smaller and flattened minimum observed in n around T_C for the MA-sample with respect to the RQ-sample.

ACKNOWLEDGMENTS

This work was supported by the Spanish Ministry of Science and Innovation (MICINN) and EU FEDER (Project No. MAT2010-20537), the PAI of the Regional Government of Andalucía (RGA) (Project No. P10-FQM-6462) and the United States Office of Naval Research (Project No. N00014-11-1-0311). L. M. Moreno acknowledges a research internship funded by MICINN. J. J. Ipus acknowledges a research contract from RGA.

¹R. Alben, J. J. Becker, and M. Chi, *J. Appl. Phys.* **49**, 1653 (1978).

²G. Herzer, *IEEE Trans. Magn.* **26**, 1397 (1990).

³A. Hernando *et al.*, *Phys. Rev. B* **51**, 3581 (1995).

⁴M. E. McHenry *et al.*, *Prog. Mater. Sci.* **44**, 291 (1999).

⁵V. Franco *et al.*, *Annu. Rev. Mater. Res.* **42**, 305 (2012).

⁶C. Suryanarayana, *Prog. Mater. Sci.* **46**, 1 (2001).

⁷L. M. Moreno *et al.*, *J. Alloys Compd.* **585**, 485 (2014).

⁸J. M. Borrego *et al.*, *J. Appl. Phys.* **92**, 6607 (2002).

⁹H. P. J. Wijn, *Landolt-Börnstein Neue serie: Magnetische Eigenschaften von Metallen* (Springer-Verlag, Berlin-Heidelberg, 1991), Vol. 19, p. 126.

¹⁰V. Franco *et al.*, *J. Appl. Phys.* **101**, 09C503 (2007).

¹¹V. Franco, J. S. Blázquez, and A. Conde, *Appl. Phys. Lett.* **89**, 222512 (2006).

¹²J. J. Ipus *et al.*, *J. Alloys Compd.* **496**, 7 (2010).

¹³J. J. Ipus *et al.*, *J. Appl. Phys.* **105**, 123922 (2009).

¹⁴R. Caballero-Flores *et al.*, *J. Appl. Phys.* **105**, 07A919 (2009).